Hindawi
Journal of Advanced Transportation
Volume 2023, Article ID 9744737, 14 pages
https://doi.org/10.1155/2023/9744737

Research Article

Vehicle Trajectory Control and Signal Timing Optimization of Isolated Intersection under V2X Environment

Yazhu Zou, Moyan Li, Jiabo Guo, Enjian Yao, and Rongsheng Chen

School of Traffic and Transportation, Beijing Jiaotong University, Beijing 100044, China

Correspondence should be addressed to Yazhu Zou; 20251229@bjtu.edu.cn

Received 11 January 2023; Revised 8 March 2023; Accepted 25 May 2023; Published 22 June 2023

Academic Editor: Ziyuan Pu

This study proposes a two-level optimization model system for vehicle control and signal timing at isolated signal intersections under the mixed traffic flow environment composed of intelligent connected autonomous vehicles (CAVs) and connected human-driven vehicles (CHVs), to minimize the energy consumption and vehicle delay at intersections. The proposed two-layer optimization model is composed of a two-layer vehicle trajectory control model and a fuzzy control signal timing optimization model. The two-layer vehicle trajectory control model includes a signal-oriented vehicle trajectory control model and a car-following oriented vehicle trajectory control model. The former calculates expected acceleration and speed commands at each time step according to the coming signal information, to help vehicle pass the closest signal intersection without stopping during the green light interval; the latter uses the variable headway (VTH) strategy to follow the preceding vehicle by maintaining a safe distance. A microscopic simulator based on SUMO is developed to test the performance of the proposed optimization algorithm. In the simulation experiment, with the driving characteristics of CHV drivers considered, the results show that our model performs well under a CAV penetration rate of 30%–60% and under small or moderate levels of traffic flow. The average waiting time of vehicles is reduced by about 25% compared with the uncontrolled scheme. Under the condition of penetration rate of 60%, the average energy consumption of vehicles in the proposed model is 17.56% lower than that of the uncontrolled scheme. In addition, the proposed model reduces by 21.94% compared with the scheme of only controlling vehicles. When the traffic flow is at a low or medium level, the average energy consumption and waiting time of vehicles are reduced by nearly 35% with the proposed model.

1. Introduction

In recent years, intelligent transportation and transportation big data have developed rapidly. For a long time to come, the traffic flow on the road will include both traditional manual driving vehicles and connected and autonomous vehicles (CAVs). It will be a big trend to transition from a homogeneous flow composed of one vehicle type to a mixed traffic flow composed of at least two types. At the meanwhile, with the rapid growth of car ownership, the problem of traffic congestion has become increasingly prominent. Road intersections are often the bottleneck of urban road network traffic flow. In addition, the control of traffic lights at intersections makes vehicles at intersections accelerate and decelerate frequently, resulting in low traffic efficiency and low fuel economy. Traffic signal coordination is an important way to enhance traffic safety, to improve traffic efficiency, and to reduce traffic emissions. Traffic signal coordination is through vehicle-to-vehicle (V2V) communication and vehicle-to-infrastructure (V2I) communication to obtain information about the motion status of surrounding vehicles, as well as signal phase and timing (spit) information from signals hundreds of meters away. Through the obtained information and the trajectory optimization control combined with the signal information, the vehicle finally realizes the ecological driving of the signal intersection.

Many existing studies have conducted relevant research on the guidance, control, and signal timing of intelligent connected vehicles in the networked intersection environment.

Jiang et al. [1] evaluated the performance of ecological approach control systems at signalized intersections in partially connected and automated vehicle (CAV) environments. They tested two different networks, including an isolated signalized intersection and a corridor with two signalized intersections. The results show that the controller generally improves fuel efficiency without affecting maneuverability, and its environmental performance is affected by the lowest CAV speed, green ratio, congestion level, and sign penetration rate. Ghiasi et al. [2] proposed a CAV-based trajectory smoothing model to coordinate traffic, which could improve fuel efficiency and reduce environmental impact. This real-time control algorithm for traffic coordination is applicable to the mixed traffic environment of manual driving vehicles (HDVs), connecting vehicles (CVs), and CAVs. Yao et al. [3] proposed a two-level joint optimization framework for traffic signals and vehicle trajectories to reduce gasoline consumption and transport emissions. There are good results under different conditions of CAV permeability. Gutesa et al. [4] proposed an intersection management strategy for automated vehicle corridors based on the vehicle trajectory-driven optimization method. The automated driving trajectory driven optimization model was based on the vehicle position, traffic conditions, and signal status on the corridor to calculate the optimal trajectory for CAV, and reduced vehicle delays along the signal corridor with fixed time signal control. Guo and Ma [5] proposed a signaling corridor management framework based on CAV technology for vehicle layout and trajectory control (SCoPTO). In this framework, when vehicles on the main roads arrived at the downstream intersections in the form of a platoon, the framework could request to extend the green time to reduce unnecessary parking and improve the utilization rate of green time as much as possible and improve the traffic stability. Guo and Ma [6] proposed a real-time learning and control framework for signalized intersection management, including signal optimization and CAV trajectory control. By using efficient trajectory planning algorithms, you can control the vehicle trajectory of CAV, maximize the use of green time, and reduce the startup loss time. Lu et al. [7] proposed an ecological intelligent driver model (EcoSDM) to improve the fuel efficiency and traffic flow of vehicles by adjusting the speed of leading vehicles in fleets. Yi et al. [8] had established a hybrid equilibrium model for CAV platoon and human-driven vehicle (HDV), taking into account both the positive and negative aspects of CAV platoon. In addition, the study proposes an optimal path layout method that integrates the travel costs of CAV and HDV into its objective function to reduce negative defects. The numerical results indicate that introducing CAV platoons may increase initial travel costs, and this method can effectively reduce platform disturbance interference, thereby promoting the widespread application of CAV platoons. Hea and Wu [9] proposed an optimal control model that utilizes promising connected vehicle technology and proposes two eco-driving consulting strategies. The model better solves the problem of reducing the energy consumption of all vehicles when traditional gasoline vehicles (GVs) and electric vehicles (EVs) form a platoon that is considered energy friendly transportation mode. The results of numerical experiments show that it is important for eco-driving consulting system to consider the energy consumption characteristics of the vehicle as a whole. Gong and Du [10] have developed a coordinated control algorithm of CAV and HDV to ensure the smoothness and stability of system level traffic flow, as well as the mobility and safety of individual vehicles. Long et al. [11] proposed a comprehensive optimization method based on traffic signals and vehicle motion tracks. Wang et al. [12] described a co-operative ecology-driven (CED) system for signal corridors, focusing on how the penetration rate of CAVs affects the energy efficiency of transport networks. In addition, they proposed a role switching protocol that lets CAVs switch between the leader and subsequent vehicles in the string. Aiming at traditional vehicles and different cabs in the network, a longitudinal control model is developed according to their roles and distance from the intersection. PTV VISSIM simulation results show that with the increase of CAV penetration, the energy consumption and pollutant emissions of the system decrease gradually. When all vehicles in the proposed system are CAVs, energy consumption can be reduced by more than 7 percent and pollutant emissions by more than 59 percent. Pourmehrab et al. [13] compared two state-of-the-art intersection management algorithms (IMAs) for CAVs and conventional vehicles (CNVs), as well as an actuated signal control system (ASCS). Two IMAs are adopted, Intelligent Intersection Control Algorithm (IICA) and Hybrid Autonomous Intersection Management (H-AIM), to improve the efficiency of intersections through vehicle automation and connectivity. Berbar et al. [14] proposed a dual agent (DA) intelligent traffic signal module control based on the reinforcement learning (RL) method. The speed agent (VA) aimed to minimize fuel consumption by controlling the speed of the platoon and single CAVs crossing the signal intersection and effectively reduce traffic delay through signal sequencing and phases. Zhou et al. [15] proposed a vehicle tracking model based on reinforcement learning to obtain appropriate driving behavior and to improve the driving efficiency, fuel consumption, and safety of signalized intersections in real time. Yao et al. [16] evaluated the impact of connected and autonomous vehicles on fuel consumption and emissions of mixed traffic flow on highways. Three following models were used to capture the following behavior in mixed traffic flow. The effects of connected and autonomous vehicles on fuel consumption and traffic emissions of mixed traffic flow were studied through numerical simulation. Finally, some factors affecting fuel consumption and traffic emissions of mixed traffic flow were discussed. The simulation results show that networked automated vehicles can significantly reduce fuel consumption and transportation emissions. Nie and Farzaneh [17] proposed a real-time dynamic predictive cruise control (PCC) system. In the comprehensive traffic situation of the comprehensive driving scene, the constraints of the previous vehicle and the influence of traffic lights are considered to improve the driving performance of the vehicle.

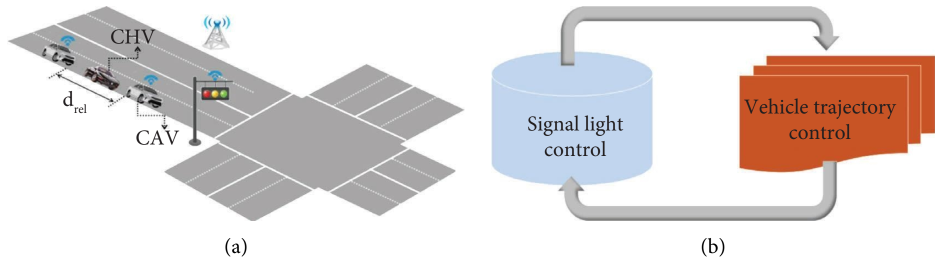

Figure 1: Double-layer model predictive control system.

It can be seen from the above studies that most of the previous studies focused on controlling the vehicle's trajectory to achieve the minimum fuel consumption, or controlling the vehicle's trajectory to achieve the highest traffic efficiency at the signalized intersection, or comprehensively considering the vehicle's energy consumption and traffic efficiency at the intersection. However, most of the studies that comprehensively consider the above two objectives are achieved by controlling the signal phase and timing of the signalized intersection or jointly controlling the vehicle trajectory and the timing and phase of the signalized intersection, but the method is relatively simple. Most of them did not consider the impact of different types of drivers and the differences of CAV car-following behavior in different situations. Therefore, the goal of this paper is to develop an intersection control optimizer based on the secondary development of SUMO using Python according to different driving situations and the uncertainty brought by manual driving vehicles:

(1) A mixed traffic flow driving situation (which can be realized in the real world in the near future) is constructed to comprehensively consider the minimization of vehicle delay and vehicle energy consumption, so as to realize the comprehensive optimization applicable to isolated signalized intersections.
(2) A two-level model predictive control system for vehicles is proposed to distinguish driving scenarios through switching logic algorithm to realize recognition, classification, and control of vehicle driving status. The vehicle two-level model predictive control system mainly includes two parts: the vehicle trajectory control model based on signal and the vehicle trajectory control model oriented to car-following.
(3) The randomness of Connected Human-Driven Vehicle (CHV) is considered in the SUMO simulation process.
(4) The fuzzy control algorithm is proposed to optimize the signal phase duration. Under the driving situation of mixed traffic flow (which can be realized in the real world in the near future), the minimization of vehicle delay and vehicle energy consumption shall be comprehensively considered to achieve the comprehensive optimization applicable to isolated signal intersections.

2. Methods

2.1. Environment Construction of Mixed Connected Automated Vehicle Signal-Controlled Intersection. This paper designs a bidirectional four-lane cross-intersection scene, as shown in Figure 1. The two types of vehicles in the scenario are CAV and CHV, both of which have network communication capabilities. CAV is a fully autonomous vehicle with intelligent sensing, decision-making, and control capabilities. CAV also can communicate with other vehicles or traffic lights. CHV can communicate with nearby vehicle V2V. Traffic lights at intersections also have network communication capabilities, which can realize V2I communication with vehicles in the scene.

In addition, in order to focus on the problem, this paper makes the following assumptions:

(1) Before entering the intersection area, vehicles do not change lanes, reverse, turn around, and other behaviors. Only the straight behaviors of vehicles entering the intersection area are considered and follow the principle of first-come first reservation.
(2) The effective communication range of V2I is within 400 m of connected traffic lights (central point of intersection). When vehicles enter the effective communication range of signal lights, CAV shall obey the intersection control and CHV will obey the intersection control with a certain probability. The network communication is set as real-time and reliable communication, without considering the potential network packet loss, delay, and other unreliable network conditions.
(3) Vehicles entering the intersection control range can obtain the position, speed, and other state information of surrounding vehicles by V2V and the phase information of connected traffic lights by V2I.

2.2. Problem Formulation and System Modeling

2.2.1. Construction of Vehicle Double-Layer Model Predictive Control System. This paper aims to develop a real-time predictive control system for vehicles to minimize the energy consumption of vehicles in urban traffic systems and improve the efficiency of crossing traffic, taking into account the constraints of preceding vehicles and the influence of traffic lights. The method is shown in Figure 1. d_{rel} indicates the distance between the controlled vehicle and the vehicle in front; d_{TL} indicates the relative distance to an upcoming signalized intersection.

For vehicles on the road, we divide them into affected CAVs and unaffected CAVs according to whether they are affected by the preceding vehicle. The signal-based vehicle trajectory control model described in 3.1.1 is implemented for the CAV that is not affected by the preceding vehicle, and the trajectory control model based on car-following behavior established in Section (1) is implemented for the affected CAV.

(1) Signal-Based Vehicle Trajectory Control Model. In the context of vehicle-road coordination, CAVs can conduct real-time two-way wireless communication with traffic infrastructure (such as traffic lights) and perceive and obtain relevant information about the surrounding environment. If CAVs detect the presence of vehicles in front of them, CAVs should adjust the vehicle trajectory by the vehicle trajectory control model oriented to real-time traffic signal information optimization at this moment, to cross the upcoming signal intersection at the green light time. The optimal control command of CAVs is calculated based on real-time traffic signal information, and the optimal control strategy is used to minimize the energy consumption when vehicles pass through the signalized intersection. The objective function of the signal-based vehicle control algorithm is as follows:

$$\min \sum_{i=k}^{k+N_e-1} \left(E\left(v_{\text{host},i}, a_{\text{host},i}, T_{m,i}\right) + \varphi_1 \left(v_{\text{host},i} - v_{\text{target}}\right)^2 + \varphi_2 \varepsilon_{1,i}^2 + \varphi_3 \varepsilon_{2,i}^2 \right), \tag{1}$$

wherein $E(v_{\text{host},i}, a_{\text{host},i}, T_{m,i})$ represents the energy consumption of the vehicle, v_{target} represents the target vehicle speed optimized based on signal phase information, and $\varepsilon_{1,i}$ and $\varepsilon_{2,i}$ are relaxation variables. φ_1, φ_2, and φ_3 are weighting factors, respectively. From this, it can be seen that the vehicle control model based on signal consists of four parts to control different targets. The first goal is to minimize the energy consumption of vehicles passing through the intersection. However, we consider that if only the first term exists as our objective function, the vehicle will stop at the intersection, because the first term forces the vehicle to consume as little energy as possible. When the vehicle stops, the vehicle will consume the least energy. Therefore, in order to avoid this phenomenon, we introduced the second term to punish the difference between the vehicle speed and the reference target vehicle speed, so that the vehicle can be as close as possible to the reference target speed to further minimize the energy consumption. The third item penalizes ε_1 the slack variable to force the vehicle as close to the stop bar as possible, while stopping appropriately within the red interval. The fourth item is introduced with relaxation variables ε_2 to minimize the derivative of acceleration to ensure driving comfort.

s.t.

$$v_{\text{host},i+1} = v_{\text{host},i} + \frac{1}{\text{meq}} \begin{bmatrix} i_g \bullet \eta_e \bullet \dfrac{T_{m,i}}{r_w} - c_r \bullet m_{eq} \bullet g \bullet \cos\theta_i \\ -\dfrac{1}{2} \bullet \rho_a \bullet A_f \bullet C_D \bullet {v_{\text{host},i}}^2 - m_{eq} \bullet g \bullet \sin\theta_i \end{bmatrix}, \tag{2}$$

$$d_{TL,i+1} = d_{TL,i} - \frac{v_{\text{host},i} + v_{\text{host},i+1}}{2}, \tag{3}$$

$$0 \le d_{TL,i} \le d_{TL,\max} + \varepsilon_{1,i}, \tag{4}$$

$$v_{\min,i} \le v_{\text{host},i} \le v_{\max,i}, \tag{5}$$

$$a_{\min,i} \le a_{\text{host},i} \le a_{\max,i}, \tag{6}$$

$$j_{\min,i} - \varepsilon_{2,i} \le a_{\text{host},i+1} - a_{\text{host},i} \le j_{\max,i} + \varepsilon_{2,i}, \tag{7}$$

$$0 \le T_{m,i} \le T_{m,\max}. \tag{8}$$

The speed of the driving vehicle is calculated through constraint (2), where m_{eq} is the total mass of the vehicle, i_g is the single transmission ratio, η_e is the total mechanical efficiency of the transmissions system, r_w is the wheel radius, c_r is the rolling resistance coefficient, g is the gravity acceleration, θ is the road slope, ρ_a is the air density, A_f is the front area of the vehicle, and C_D is the air resistance coefficient. Constraint (3) obtains the distance from the signal intersection, and the soft constraint (4) is used to avoid active parking away from the signal intersection. The vehicle speed is limited in constraint (5).The vehicle acceleration, deceleration, and motor torque are limited by the technical characteristics of the vehicle itself to constrain (7) to (8).

After solving the above optimization problem in each time step, the specific control strategy of the vehicle can be obtained. The vehicle is controlled and SUMO simulated by the control strategy. Then, the above process is repeated for the next controllable vehicle, namely, CAV, to achieve the real-time update of vehicle status at the whole intersection and achieve the goal of minimizing vehicle energy consumption at the intersection by continuously repeating the signal-based vehicle control algorithm.

(2) A Car-Following Oriented Vehicle Trajectory Control Model. If the presence of the vehicle ahead is detected by CAVs, CAVs should follow the vehicle in front of it, while

maintaining a safe distance from the vehicle in front and achieving a higher road resource utilization rate. In this case, a car-following oriented vehicle trajectory control model is adopted, which is developed to manage the traffic scene of the previous vehicle within the detection range of the vehicle sensor.

The objective function of this control algorithm is as follows:

$$\min \sum_{i=k}^{k+N_e-1} \begin{pmatrix} E\left(v_{\text{host},i}, a_{\text{host},i}, T_{m,i}, \omega_{m,i}\right)+, \\ \varphi_1 \varepsilon_{1,i}^2 + \varphi_2 \varepsilon_{2,i}^2 + \varphi_3 \varepsilon_{3,i}^2 \end{pmatrix}, \tag{9}$$

s.t.

$$v_{\text{host},i+1} = v_{\text{host},i} + \frac{1}{m_{eq}} \begin{bmatrix} i_g \bullet \eta_e \bullet \dfrac{T_{m,i}}{r_w} - c_r \bullet m_{eq} \bullet g \bullet \cos\theta_i \\ -\dfrac{1}{2} \bullet \rho_a \bullet A_f \bullet C_D \bullet v_{\text{host},i}^2 \\ -m_{eq} \bullet g \bullet \sin\theta_i \end{bmatrix}, \tag{10}$$

$$d_{TL,i+1} = d_{TL,i} - \frac{v_{\text{host},i} + v_{\text{host},i+1}}{2}, \tag{11}$$

$$0 \le d_{TL,i} \le d_{TL,\max} + \varepsilon_{1,i}, \tag{12}$$

$$v_{\min,i} \le v_{\text{host},i} \le v_{\max,i}, \tag{13}$$

$$\begin{aligned} a_{\min,i} &\le a_{\text{host},i} \le a_{\max,i}, \\ j_{\min,i} - \varepsilon_{2,i} &\le a_{\text{host},i+1} - a_{\text{host},i} \le j_{\max,i} - \varepsilon_{2,i}, \end{aligned} \tag{14}$$

$$0 \le T_{m,i} \le T_{m,\max}, \tag{15}$$

$$0 \le \omega_{m,i} \le \omega_{m,\max}, \tag{16}$$

$$v_{\text{rel},i} = v_{\text{preceding},i} - v_{\text{host},i}, \tag{17}$$

$$D_{\text{safe},i} = \tau_1 \bullet v_{\text{host},i} + \tau_2 \bullet v_{\text{host},i}^2 - \tau_3 \bullet v_{\text{rel},i} \bullet v_{\text{host},i} + d_{\min}, \tag{18}$$

$$d_{\text{rel},i} + \begin{pmatrix} \dfrac{v_{\text{preceding},i} + v_{\text{preceding},i+1}}{2} \\ -\dfrac{v_{\text{host},i} + v_{\text{host},i+1}}{2} \end{pmatrix}, \tag{19}$$

$$D_{\text{safe},i} \le d_{\text{rel},i} \le D_{\text{safe},i} + \varepsilon_{3,i}. \tag{20}$$

In constraint (9), ε_3 is a relaxation variable; D_{safe} refers to the dynamic safety distance between the CAV and the previous vehicle; $d_{\min}$ refers to the minimum distance between two vehicles at rest; and τ_1, τ_2, and τ_3 are all constant values greater than zero. A car-following oriented vehicle trajectory control model has similar objectives as the previous problem. During vehicle following, the speed of CAV approaching the reference target speed is not constrained, but another relaxation variable ε_3 is introduced, in order to maintain a safe distance between the CAV and the previous vehicle during following. According to constraint (18), we can calculate the relative speed between two cars, and the dynamic safe distance between two vehicles is calculated by constraint (19). The real-time relative distance model is calculated by constraint (20). Constraint (21) ensures driving safety and includes a soft constraint that pushes the CAV forward to achieve subsequent functions. Once the distance between them is greater than D_{safe}, the relaxation variable ε_3 is increased to make the CAV drive faster.

Considering driving safety and road utilization, the safe distance between the CAV and the previous vehicle is calculated as follows:

$$D_{\text{safe}} = \text{CTH} \bullet v_{\text{host}} + d_{\min}, \tag{21}$$

where CTH represents the time progression of a constant.

Instead of using constant time interval (CTH), a customized variable time interval (VTH) strategy is designed in this paper, which not only considers the speed of the CAV but also the relative speed between the CAV and the previous vehicle, which is expressed as follows:

$$\begin{aligned} \text{VTH} &= \tau_1 + \tau_2 \bullet v_{\text{host}} - \tau_3 \bullet v_{\text{rel}}, \\ v_{\text{rel}} &= v_{\text{preceding}} - v_{\text{host}}, \end{aligned} \tag{22}$$

where v_{rel} is the relative speed between CAV and the vehicle in front of it; τ_1, τ_2, and τ_3 are constants greater than 0. By replacing CTH with VTH in the above expression, the adaptive safe distance can be obtained:

$$\begin{aligned} D_{\text{safe}} &= \text{VTH} \bullet v_{\text{host}} + d_{\min} \\ &= \tau_1 \bullet v_{\text{host}} + \tau_2 \bullet v_{\text{host}}^2 - \tau_3 \bullet v_{\text{rel}} \bullet v_{\text{host}} + d_{\min}. \end{aligned} \tag{23}$$

(3) Switching Logic Algorithm. The core functional module consists of two linear model predictive controllers, namely, the signal-based vehicle trajectory control model and the car-following behavior-based vehicle trajectory control model. Both controllers calculate the optimal control instruction u at each time step as the input of the CAV. In the context of vehicle-road coordination, the instantaneous output of the CAV can be obtained, including its speed v_{host}, the distance between vehicles d_{rel}, and the relative distance to the nearest signalized intersection d_{TL}, as well as phase and time information of real-time traffic lights, speed of the vehicle ahead v_{pre}, and the speed limit of certain road sections v_{limits}, and these information are fed into the switch logic algorithm to correctly select one of the two vehicle trajectory control models. The specific control process is shown in Figure 2.

The specific control logic is as follows:

The detected sensor d_{rel} is compared with a limit value d_{limit}.

If d_{rel} is not greater than d_{limit}, then select the vehicle trajectory control model based on car-following behavior to control the CAV to follow the vehicle in front.

If d_{rel} is not less than d_{limit}, then based on a customized variable time interval strategy, a vehicle trajectory control model based on car-following behavior will be selected to

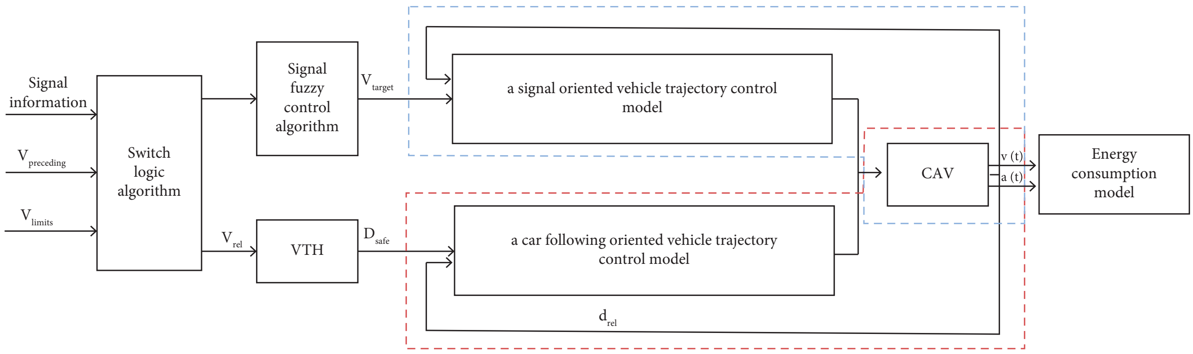

Figure 2: Schematic diagram of data flow in two-layer model predictive control system under switching logic.

maintain a safe, comfortable, and efficient road resource usage distance between vehicles.

Therefore, the vehicle trajectory control of the CAV in different driving states can be realized through the switch logic algorithm, thereby achieving the goal of minimizing energy consumption.

(4) Signal Fuzzy Control Algorithm. Set detection points in each lane of the intersection, place detectors, and transmit the detected vehicle data arriving at the intersection to the control system. The system controls the timing strategy of each phase and then sends these timing data to the signal lights for timing.

This paper studies the traffic signal control of a single intersection. There are three directions of traffic flow: left turn, straight ahead, and right turn at the four entrances. The signal timing diagram represents the signal timing scheme. This paper adopts the two-phase signal timing diagram, as shown in Figure 3, and the phase sequence of the signal lights is switched according to the phase sequence in the diagram.

Fuzzy control algorithm is an effective way to solve signal timing optimization at signal intersections, so this paper plans to use the fuzzy control algorithm to optimize intersection signals. Among them, this paper refers to the literature [18] and optimizes the idea of the fuzzy control system as follows: the observation module obtains vehicle queuing information and traffic arrival situation according to various detection equipment, calculates the traffic intensity of the current phase and the next phase, and compares the traffic intensity of the two phases The traffic intensity is input to the decision-making module, and before the green time of the current green-light phase ends, the decision-making module determines the green-light extension time of the current green-light phase.

Therefore, we take the number of queuing vehicles and vehicle arrival rate as the input of the observation module and take the traffic intensity of the evaluated phase as the output of the module.

The specific traffic signal control algorithm is as follows:

(1) Step 1: Give the phase that is currently allowed to pass the shortest green light time $g_{\min}$.

(2) Step 2: Before the end of the green time of the current green light phase, input the vehicle queuing information and traffic arrival information of the current green light phase and the next green light phase into the observation module and obtain the traffic intensity of the two phases through fuzzy reasoning.

(3) Step 3: Input the current green light phase and the next green light phase intensity into the decision-making module and obtain the green light extension time of the current green light phase through fuzzy reasoning. If the extension time is >8 s and $g_{\text{duration}} + \text{extension time} < g_{\max}$, then the current green light phase extends the time and go to step 2; if the extension time > 8 s and $g_{\text{duration}} + \text{extension time} \geq g_{\max}$, go to step 4; if the extension time ≤ 8 s, go to step 5.

(4) Step 4: After the green light of the current phase is extended $(g_{\max} - g_{\text{duration}})$ and then switched to the next green light phase, go to step 5.

(5) Step 5: Switch to the next green light phase after the yellow light lasts for g_{yellow}, and go to step 1.

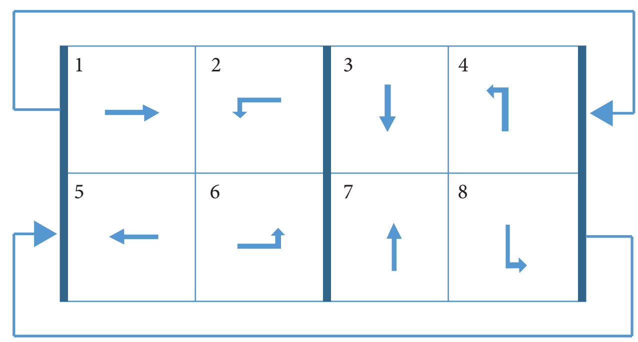

Figure 3: Two-phase signal timing diagram. (a). First phase. (b). Second phase.

Among them, $g_{\min}$ indicates the minimum green light time; $g_{\max}$ indicates the maximum green light time; g_{duration} indicates the current phase to last the green light time; and g_{yellow} indicates the yellow light time. Its unit is second (s).

The structure of the fuzzy control system in this paper is shown in Figure 4. The fuzzy control system includes an observation module and a decision module. The observation module evaluates the traffic intensity of the current phase and the next phase. The decision module determines the green light extension time of the current green light phase according to the current green light phase traffic intensity and the next green light phase traffic intensity.

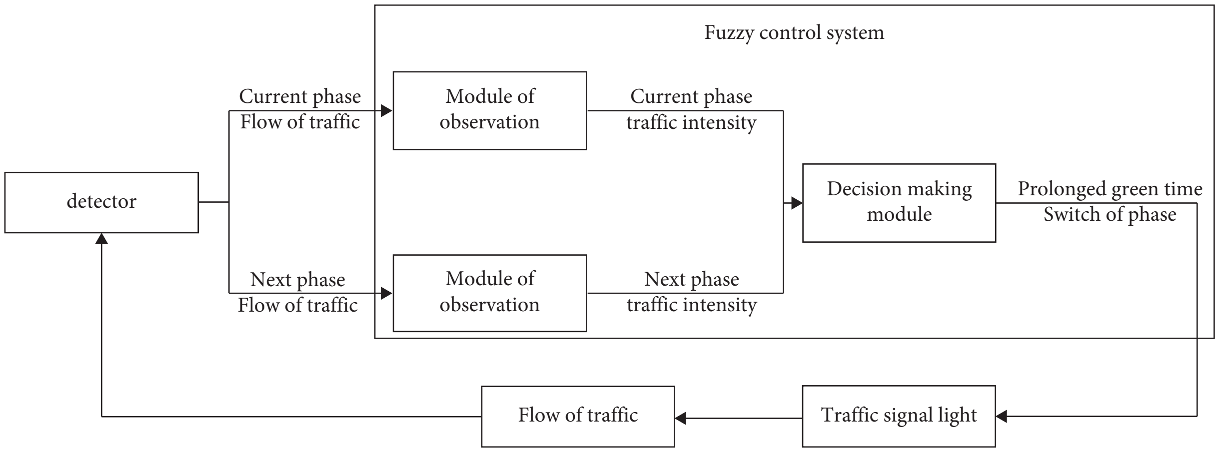

Figure 4: Structure of the fuzzy control system.

(1) Observation module

The observation module calculates the traffic intensity of the current green light phase and the next green light phase according to the detected real-time traffic flow. This module has two input variables, the number of queuing vehicles between the upstream and downstream detectors of the evaluated phase and the vehicle arrival rate of the phase, and the output variable is the traffic intensity of the evaluated phase. Vehicle arrival rate, the number of vehicles arriving at an intersection approach lane per second, is calculated from the number of vehicles arriving in a cycle measured by a lane checker. The discourse domain of the number of queuing vehicles is set to [0, 20], where it can be divided into five fuzzy subsets: {few, few, medium, many, many}, abbreviated as {NS, S, M, L, PL}; the membership function of each subset is shown in Figure 5. The domain of vehicle arrival rate is set to [0, 1], which is divided into five fuzzy subsets: {very low, low, medium, high, very high}, abbreviated as {NS, S, Z, M, PM}.

The domain of traffic intensity is [0, 6], divided into five fuzzy subsets: {very low, low, medium, high, very high}, abbreviated as {VD, D, M, U, VU}; see Table 1 for the fuzzy rules.

(2) Decision-making module

The decision-making module determines the green light extension time of the current green light phase according to the current phase traffic intensity and the next phase traffic intensity. This module has two input variables, which are the current phase traffic intensity and the next phase traffic intensity, and the output variable is the current green light phase extension time. The fuzzy subset division of the current phase traffic intensity and the next phase traffic intensity is the same as before. The extended time domain is [0, 30], divided into 5 fuzzy subsets: {very short, short, medium, long, very long}, abbreviated as {NS, S, M, L, PL}; see Table 2 for the fuzzy rules.

(3) Fuzzy reasoning and reconciliation fuzzification

Fuzzy reasoning is based on the input fuzzy number, controlled by fuzzy rules to complete fuzzy reasoning to solve fuzzy relational equations. The fuzzy control system designed in this paper adopts the product inference method and center of gravity method to defuzzify. The exact calculation method of the center of gravity method is shown in the following formula:

$$u^* = \frac{\sum_{i=1}^{I}(u_i \mu_i)}{\sum_{i=1}^{I}\mu_i}, \quad (24)$$

In the formula, u^* is the precise output of the decision result; u_i is the central value of the consequent membership function of the i-th fuzzy rule triggered; μ_i is the product of the membership degrees of all input variables of the i-th rule being triggered; and I is the number of triggered fuzzy rules.

(5) Energy Consumption Model. The energy consumption model of a vehicle is usually related to speed or acceleration. And when we control the vehicle, we mainly control the speed and acceleration of the vehicle. Therefore, we choose an energy consumption model related to speed and acceleration to calculate the total energy consumption of vehicles at the intersection. This paper plans to adopt the instantaneous gasoline consumption function proposed by Akcelik (1989) because it takes acceleration and velocity into account. The gasoline consumption rate is calculated based on the instantaneous speed and acceleration of the vehicle.

The specific model is as follows:

$$F(v, a, t) = \left[\alpha + \beta_1 P(t) + \beta_2 m_{eq} a(t)^2 v(t)\right]_{a>0},$$
$$P(t) = \max\left\{\begin{array}{c} 0, d_1 v(t) + d_2 v(t)^2 + d_3 v(t)^3, \\ \\ +\dfrac{m_{eq}}{1000} a(t) v(t). \end{array}\right\}, \quad (25)$$

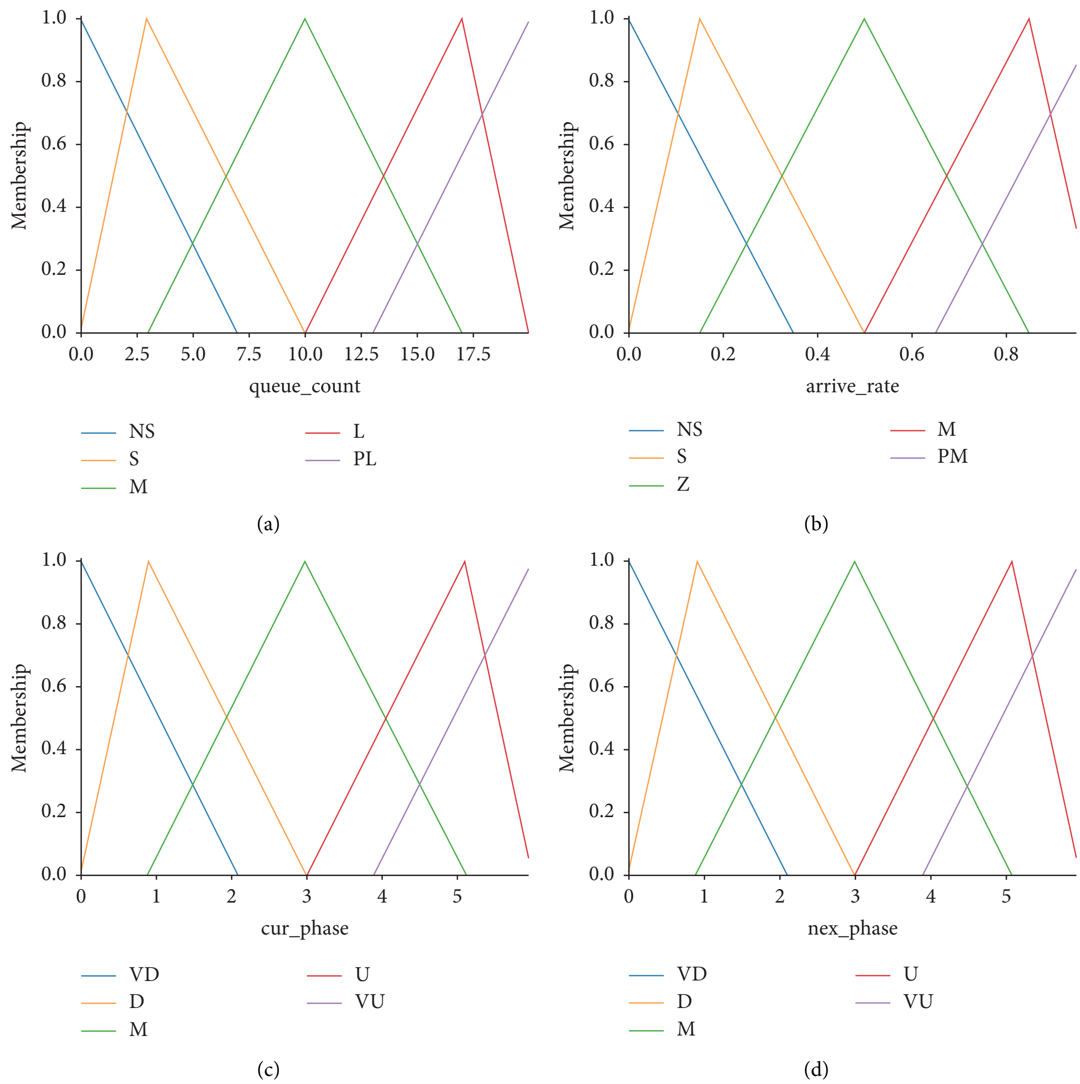

Figure 5: Membership function of (a) the number of queued vehicles, (b) arrival rate, (c) current phase, and (d) next phase.

Table 1: Fuzzy rules of the observation module.

Traffic intensity		Vehicle arrival rate				
		NS	S	Z	M	PM
Queuing vehicles	NS	VD	D	M	U	U
	S	VD	D	M	U	VU
	M	D	M	M	U	VU
	L	D	M	M	VU	VU
	PL	D	M	U	VU	VU

Table 2: Fuzzy rules of the decision module.

Extension of time		Current phase traffic intensity				
		VD	D	M	U	VU
Next phase traffic intensity	VD	NS	NS	NS	NS	NS
	D	S	S	NS	NS	NS
	M	M	L	M	S	S
	U	PL	L	L	M	S
	VU	PL	PL	PL	L	M

where α is the constant idle gasoline consumption rate (mL/s), β_1 is an efficiency parameter related to engine efficiency (mL/KJ), β_2 is the positive acceleration (mL/KJ • m/s^2) related to gasoline consumption parameters, v is the vehicle speed, and a is the vehicle acceleration. P represents the total power of the vehicle running (KW), (mL/KJ) is the rolling resistance, d_2 is the engine drag coefficient, and d_3 is the air drag coefficient.

Referring to Akcelik (1989) for parameter values, $d_1 = 0.269$, $d_2 = 0.0171$, $d_3 = 0.000672$, $\beta_1 = 0.072$, $\beta_2 = 0.0344$, and $\alpha = 0.666$.

(6) Description of Driving Behavior of Manual Driving Vehicle. In this paper, a random vehicle tracking model, the improved two-dimensional intelligent driver model, is used to capture the random driving behavior of CHV. Due to the

randomness of the vehicle tracking model we choose, the vehicle's motion trajectory will be different in different operations. Therefore, the following model can better solve the uncertain behavior of manual driving vehicles and reflect the difference of driving behavior of manual driving vehicles [19]. See Table 3 for the meaning of parameters in the above formula.

$$
\begin{aligned}
a_n^{2D-IDM}(t) &= a\left(1-\left(\frac{v_n(t)}{v_{\lim}}\right)^4-\left(\frac{d_{\text{desired},n}^{\text{2D-IDM}}(t)}{d_n(t)}\right)^2\right),\\
d_{\text{desired},n}^{\text{2D-IDM}}(t) &= s_0+\max\left(\begin{array}{c} v_n(t)T_{\text{desired},n}(t),\\ +\dfrac{v_n(t)\left(v_n(t)-v_{n-1}(t)\right)}{2\sqrt{ab}},0\end{array}\right),\\
d_n(t) &= x_{n-1}(t)-x_n(t)-lv,\\
T_{\text{target},n}(t) &= \begin{cases} T_{\min}+r\left(T_{\max}-T_{\min}\right) If r_1<p,\\ T_{\text{target},n}(t-\Delta t)\text{otherwise},\end{cases}\\
T_{\text{desired},n}(t) &= \begin{cases} T_{\text{desired},n}(t-\Delta t),\\ \text{If} T_{\text{desired},n}(t-\Delta t)=T_{\text{target},n}(t),\\ \max\left(T_{\text{desired},n}(t-\Delta t)-\Delta T, T_{\text{target},n}(t)\right),\\ \text{If } T_{\text{desired},n}(t-\Delta t)>T_{\text{target},n}(t),\\ \min\left(T_{\text{desired},n}(t-\Delta t)+\Delta T, T_{\text{target},n}(t)\right),\\ \text{If } T_{\text{desired},n}(t-\Delta t)<T_{\text{target},n}(t).\end{cases}
\end{aligned} \tag{26}
$$

Table 3: Symbols and meanings.

Notation	Explanation
n	Vehicle number
a	Maximum acceleration
b	Safety deceleration
$v_{\lim}$	Limited speed of the studied road segment
s_0	Minimum spacing gap
lv	Vehicle length
Δt	Simulation time step
$T_{\min}$	Minimum time gap in the improved 2D-IDM model
$T_{\max}$	Maximum time gap in the improved 2D-IDM model
r, r_1	Two independent uniformly distributed random numbers between 0 and 1 in the improved 2D-IDM model
p	Changing probability of target time gap in the improved 2D-IDM model
ΔT	Limit of changing rate of the desired time gap in the improved 2D-IDM model
$d_n(t)$	Spacing gap between the preceding vehicle $n-1$ and the current vehicle n
$x_n(t)$	Position of vehicle n at time t
$v_n(t)$	Velocity of vehicle n at time t
$a_n(t)$	Acceleration of vehicle n at time t
$a_n^{\text{2D-IDM}}(t)$	Acceleration of vehicle n at time t in the improved 2D-IDM model
$d_{\text{desired},n}^{\text{2D-IDM}}(t)$	Desired spacing gap of vehicle n in the improved 2D-IDM model
$T_{\text{desired},n}(t)$	Desired time gap of vehicle n at time t in the improved 2D-IDM model
$T_{\text{target},n}(t)$	Target time gap of vehicle n at time t in the improved 2D-IDM model

3. Evaluation

In order to verify the effectiveness and reliability of the proposed model and system, this paper uses Python to conduct the secondary development of SUMO simulation platform and build a simulation environment. The built test scenario is shown in Figure 6, and the setting parameters are shown in Table 4.

In the process of simulation, we fully considered the influence of the driving style of the network connected driving vehicles on the simulation effect and divided it into conservative network connected manual driving vehicles, stable network connected manual driving vehicles, and aggressive network connected manual driving vehicles. Since our control scheme is aimed at CAVs, in order to prove the inclusiveness and effectiveness of our two-layer control model under different CAV permeabilities and different vehicle flows, we used Python to carry out the secondary development of SUMO, output relevant result data, and compare SUMO self-control condition, controlling vehicle tracks, and two-layer model control. That is, the traffic efficiency and energy consumption of intersections under the three schemes of vehicle trajectory control and signal joint control. The average waiting time and average energy consumption of vehicles are selected as the evaluation and comparison indicators [20].

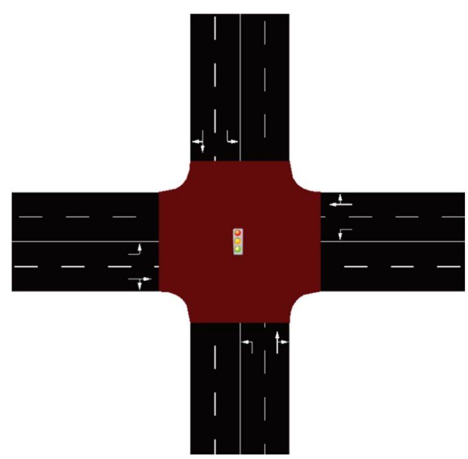

Figure 6: SUMO simulation scenario.

3.1. Comparison of Different Schemes under Different CAV Permeabilities

3.1.1. Comparative Analysis of Vehicle Energy Consumption at Intersections. Figure 7 shows the comparison of the average vehicle energy consumption of different schemes under different CAV permeabilities. The pros and cons of intersection energy consumption control under different control schemes are shown in Figure 7. Compared with the schemes with fix signal timing control and only control

Table 4: Simulation parameter setting.

Parameter	Value
Total mass of the vehicle m_{eq} (kg)	1400
Single transmission ratio i_g	2.73
Total mechanical efficiency of the transmission system η_e (%)	85
Rolling resistance coefficient c_r	0.017
Wheel radius r_w (m)	0.325
Simulation step (s)	1
Gravity acceleration g (m/s^2)	9.8
Road slope θ	1.2
Air density ρ_a (kg/m^3)	1.12256
The front area of the vehicle A_f (m^2)	2.1
Air resistance coefficient C_D	0.54
Vehicle length (m)	4.8

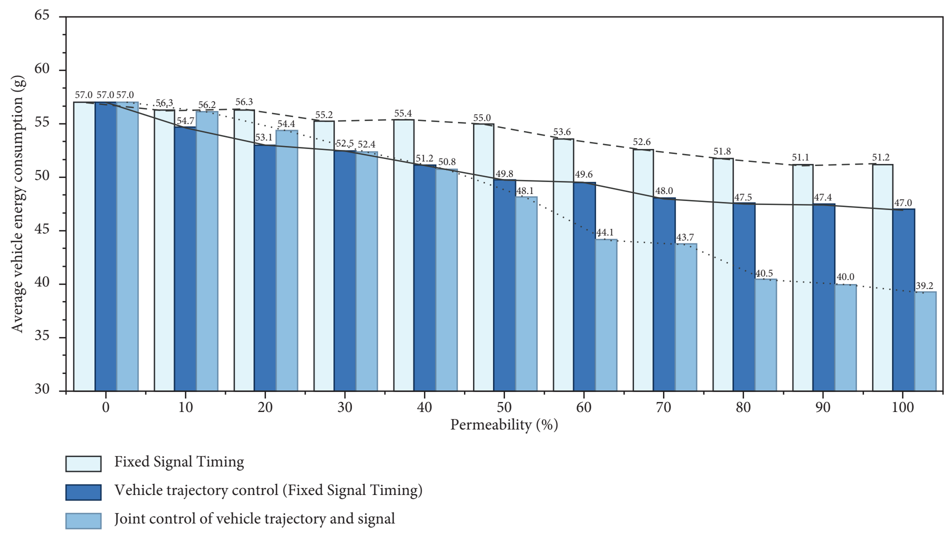

Figure 7: Comparison of average energy consumption of vehicles under different CAV permeability schemes.

vehicle trajectory, the joint control of vehicle trajectory and signal has a significant advantage.

As can be depicted from Table 5, when the permeability reaches 10%, the energy consumption saved by the joint control of vehicle trajectory and signal is −5.37% higher than that of controlling vehicle trajectory and 7.90% higher than that of no control scheme at all. At this time, due to the small amount of CAV in the road, the joint control strategy has no obvious effect on reducing the average energy consumption of the vehicle due to the influence of the randomness of the artificial vehicle driving. When the penetration rate reaches 60%, the energy consumption saved by the combined control of vehicle trajectory and signal is increased by 21.94% compared with only the control of vehicle trajectory and by 17.56% compared with the scheme of no control at all. At this time, CAVs in the road account for a large proportion. Through the control and guidance of the trajectory of CAVs, the movement trajectory of other CHVs is restricted, which avoids the phenomenon of large-scale queuing and start-stop of vehicles and thus significantly reduces the average energy consumption of vehicles at the intersection.

Table 5: Average reduction rate of vehicle energy consumption.

Penetration rate (%)	Optimization effect (average energy consumption reduction rate (%))	
	Compared to out of control	Compared to just vehicle control
10	−6.89	0.85
20	3.50	10.94
30	5.15	12.98
40	8.31	6.24
50	12.56	12.16
60	17.56	21.94
70	9.53	7.68
80	26.10	22.96
90	24.74	23.74
100	23.43	23.04

By analyzing the overall trend of the joint control scheme of vehicle trajectory and signal, it can be concluded that under this scheme, when the CAV penetration rate is between 0% and 30%, the effect of this control scheme on improving the overall energy consumption at the intersection is not very obvious. With the gradual increase of CAV permeability, the

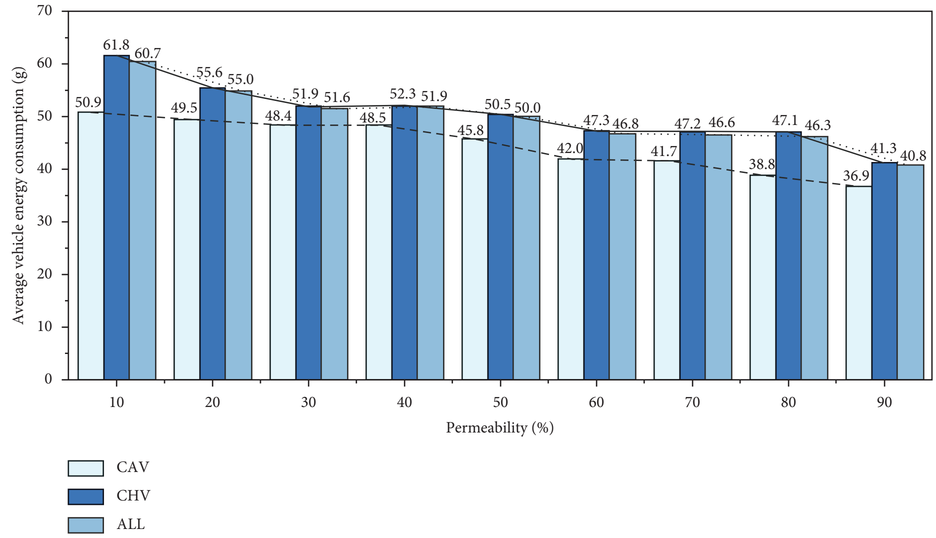

Figure 8: Comparison of the average waiting time of vehicles with two-layer control model under different CAV permeabilities.

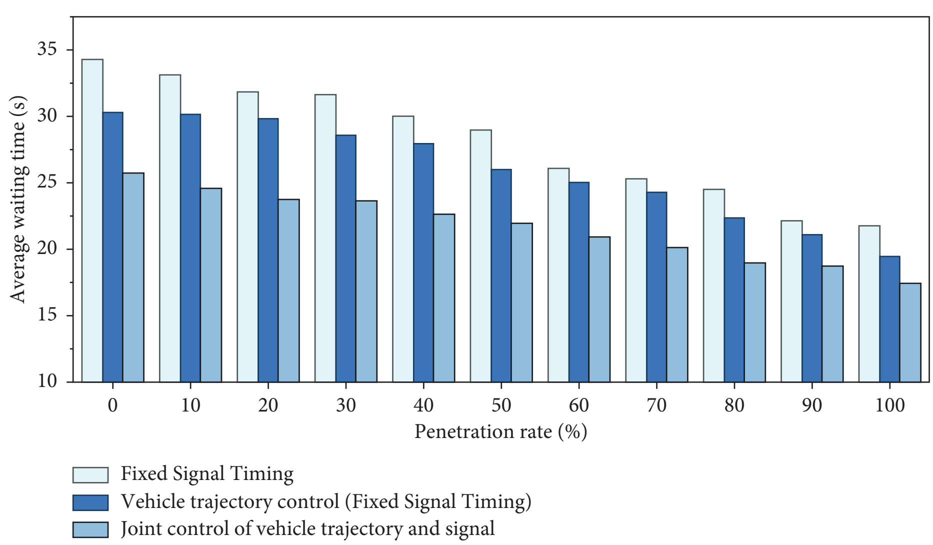

Figure 9: Comparison of average waiting time of vehicles under different CAV permeability schemes.

scheme achieved a significant improvement in the overall energy consumption at the intersection when the CAV permeability reached 30%–60%. After that, with the increase of CAV market penetration, the significance of improvement showed an insignificant or even slightly increasing trend. That is, with the increase of CAV penetration, the average energy consumption of vehicles at intersections under this control scheme did not change much. It is concluded that the control model proposed in this paper can better adapt to intersections with low and medium CAV.

Through a more detailed analysis of the simulation results, it can be concluded that when the permeability of CAV reaches 70%, the average energy consumption of vehicles at the intersection presents a slightly increasing trend. In order to better analyze the causes of this phenomenon, the average energy consumption diagram of CAV and CHVs under different CAV permeabilities under the joint control strategy of vehicle trajectory and signal was analyzed, as shown in Figure 8. It can be concluded that the reason for the slight increase in the average vehicle energy consumption at this time may be that the average vehicle energy consumption of CHVs at this time shows a trend of increasing compared with that before. Under this scenario, some CHVs may have more start-stop phenomena, resulting in the increase in the average vehicle energy consumption. Under the influence of CHV, some CAVs also show more start-stop phenomena. Thus, in this case, the average energy consumption of all vehicles presents a higher phenomenon than before.

3.1.2. Comparative Analysis of the Average Waiting Time of Vehicles at Intersections. As shown in Figure 9, the average waiting time of vehicles under different CAV permeability schemes is compared. With the increase of CAV permeability, the average waiting time of vehicles under the three control

Table 6: Reduction percentage of average waiting time of vehicles under vehicle control scheme and two-layer control model scheme.

Penetration rate (%)	Control scheme	
	Control of vehicle (%)	Signal and vehicle joint control (%)
0	11.67	24.92
10	9.06	25.81
20	6.29	25.42
30	9.49	25.30
40	6.67	24.52
50	10.33	24.46
60	3.83	19.75
70	3.95	20.50
80	8.95	22.95
90	4.52	15.63
100	10.34	19.54

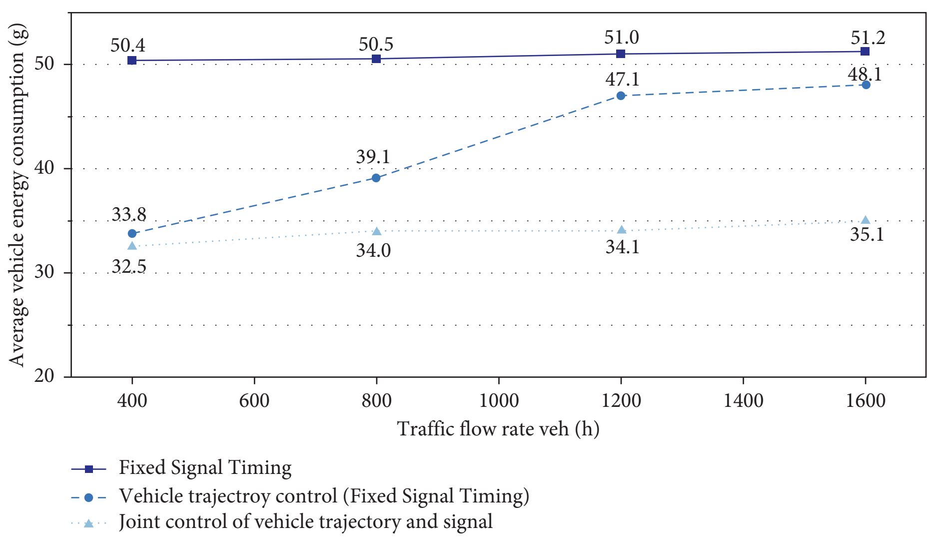

Figure 10: Average energy consumption of vehicles under different traffic volumes.

schemes shows a downward trend, which shows that our control strategy for CAV is effective. The greater the permeability of CAV, the greater the implementation of our control plan and the more comprehensive the control of intersections.

In addition, the average waiting time of vehicles under the joint control of signal and vehicles is significantly lower than the average waiting time of vehicles under the out of control and only control of the vehicle. Table 6 shows the decrease percentage of vehicle waiting time at intersections under the vehicle control scheme and the double-layer control model. It can be clearly seen that our control scheme has the best optimization effect under the conditions of medium and low permeability; with a decrease percentage of about 25%, the average waiting time of vehicles decreases greatly. With the increase of the penetration rate, the decreasing range gradually decreases. This situation is mainly caused by the following two reasons. On the one hand, it shows the uncontrollability of the manual driving of the Internet connected vehicles. According to the user equilibrium principle, all travelers look for the travel path that minimizes their travel time for their own interests, but the driving scheme determined by themselves is not necessarily the optimal scheme, and its driving track will also affect the efficiency of the whole intersection. On the other hand, it also shows that our two-layer control scheme is more suitable for the conditions where the vehicle penetration rate is at a moderate level, that is, under the conditions of mixed traffic flow, and it is highly consistent with our research background.

3.2. Index Comparison of Various Schemes under Different Traffic Volumes. In order to explore the traffic flow conditions that our two-level control model can adapt to, we compared and analyzed the operating results of each scheme under different traffic flows.

3.2.1. Comparative Analysis of Vehicle Energy Consumption at Intersections. It can be seen from Figure 10 that with the increase of traffic flow, traffic flow gradually transitions from free flow state to steady flow state, and the energy consumption of vehicles shows an upward trend. However, for the vehicle energy consumption under out-of-control scheme,

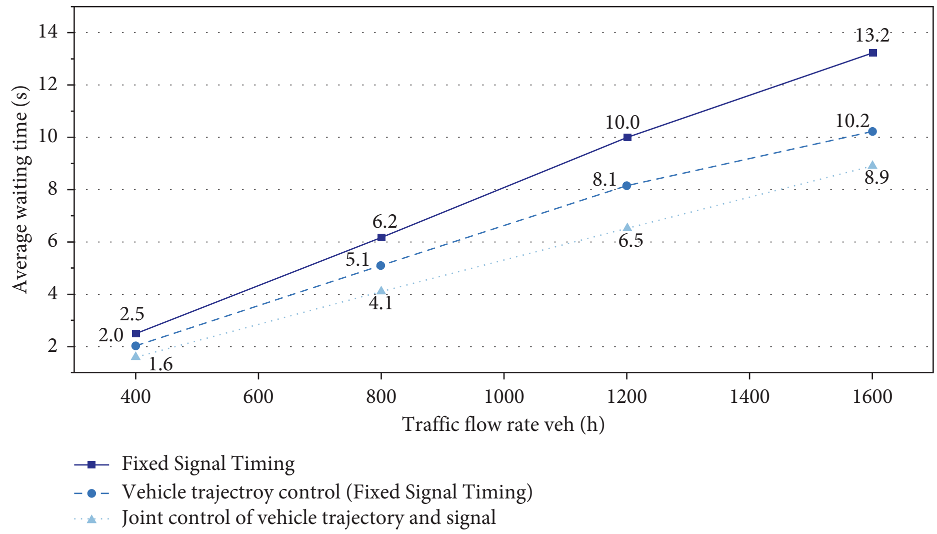

Figure 11: The average waiting time of vehicles under different traffic volumes.

since the vehicle is not controlled, the energy consumption under different traffic flows has been high, and with the increase of the traffic flow, the increase of energy consumption is not obvious. In contrast, the control of vehicle scheme and the control scheme of the double-layer model have a significant effect on the reduction of the average energy consumption of the vehicle, especially compared with the fixed signal timing scheme, the average energy consumption of the whole vehicle is reduced by about 32%. This demonstrates the effectiveness of our control scheme. Our proposed two-layer control scheme, with the increase of traffic flow, the average energy consumption of vehicles has no obvious upward trend and has always been at a low level, which also shows that our model has good stability and adaptability. The control effect is better at low and medium levels of traffic flow.

3.2.2. Comparative Analysis of Average Waiting Time of Vehicles at Intersections. It can be seen from Figure 11 that with the increase of traffic flow, the average waiting time of the three modes of out of control, control of vehicle, and signal and vehicle joint control all gradually increases. Under any level of traffic flow, vehicle trajectory control and joint control of vehicles trajectory and signal have optimization effects on the average waiting time. Among them, the signal and vehicle joint control mode has the best optimization effect on the average waiting time, and only control vehicle optimization had the second best effect on average waiting time. Let us take the flow rate of 1200 veh/h as an example. When no control is performed, the average waiting time is 10 s. When only vehicle control is performed, the average waiting time is 8.13 s, which is about 18.7% lower. The average waiting time of signal and vehicle joint control is 6.54 s, which is about 34.6% lower, and the optimization ability of the signal and vehicle joint control in the entire traffic flow range is almost unchanged. The control ability of controlling the vehicle in the middle and low traffic flow interval is almost unchanged, and the optimization ability in the high traffic flow interval is relatively enhanced. To sum up, our combined signal and vehicle control method can significantly reduce the average waiting time and improve the traffic capacity and traffic efficiency of the intersection.

4. Conclusion

To sum up, the two-layer model optimization system proposed in this paper, namely, the model of signal and vehicle joint control, has achieved good results in achieving the binocular goals of minimizing vehicle energy consumption and maximizing traffic efficiency at intersections.

Experimental simulation data show that the two-layer control model in this paper has good applicability when CAV permeability is 30%–60%, which greatly reduces the average energy consumption and average waiting time of vehicles. Compared with the no-control scheme, the average waiting time of vehicles decreases by about 25%. Under the condition of 60% permeability, the average energy consumption of the vehicle was reduced by 17.56% compared with the uncontrolled scheme and 21.94% compared with the control scheme. For the average energy consumption of vehicles, when the CAV permeability is between 0% and 30%, the scheme has a general improvement effect on the average energy consumption of vehicles. When the permeability is more than 60%, the improvement effect of the scheme has little change with the increase of the permeability, but the average energy consumption of the vehicle is significantly improved. For the average waiting time, under different permeability conditions, the average waiting time of the joint control scheme of vehicle trajectory and signal shows a downward trend, and the optimization effect is significant. Especially, when the CAV permeability is between 0% and 50%, the average waiting time of the vehicle decreases by about 25%, which is a large decrease.

In addition, the two-layer model optimization system in this paper has good applicability when the traffic flow is at a moderate level. The application of the two-layer model optimization system was able to significantly reduce the average vehicle energy consumption and the average vehicle waiting time by nearly 35 percent.

The two-layer control model proposed in this paper provides a beneficial reference scheme for the optimization of temporal and spatial resources at intersections with mixed traffic flow. At the same time, it effectively reduces the vehicle energy consumption at intersections and improves the traffic efficiency at intersections, which has strong practical significance and application value.

Data Availability

All data used to support the findings of this study are included within the article.

Conflicts of Interest

The authors declare that they have no conflicts of interest.

Acknowledgments

This study was supported by Project "Vehicle trajectory control and signal timing optimization of isolated intersection under V2X environment supported" by Beijing Jiaotong University Training Program of Innovation and Entrepreneurship for Undergraduates

References

[1] H. Jiang, J. Hu, B. B. Park, M. Wang, and W. Zhou, "An extensive investigation of an eco-approach controller under a partially connected and automated vehicle environment," *Sustainability*, vol. 11, no. 22, p. 6319, 2019.

[2] A. Ghiasi, X. Li, and J. Ma, "A mixed traffic speed harmonization model with connected autonomous vehicles," *Transportation Research Part C: Emerging Technologies*, vol. 104, pp. 210–233, 2019.

[3] Z. Yao, B. Zhao, T. Yuan, and J. Haoran, "Reduced gasoline consumption in mixed connected automated vehicles environment: a joint optimization framework for traffic signals and vehicle trajectory," *Journal of Cleaner Production*, vol. 265, 2020.

[4] S. Gutesa, J. Lee, and D. Besenski, "Development and evaluation of cooperative intersection management algorithm under connected and automated vehicles environment," *Transportation Research Record: Journal of the Transportation Research Board*, vol. 2675, no. 7, pp. 94–104, 2021.

[5] Y. Guo and J. Ma, "SCoPTO: signalized corridor management with vehicle platooning and trajectory control under connected and automated traffic environment," *Transportation Business: Transport Dynamics*, vol. 9, no. 1, pp. 673–692, 2021.

[6] Y. Guo and J. Ma, "Drl-Tp3: A learning and control framework for signalized intersections with mixed connected automated traffic," *Transportation Research Part C: Emerging Technologies*, vol. 132, 2021.

[7] C. Lu, J. Dong, L. Hu, and C. Liu, "An ecological adaptive cruise control for mixed traffic and its stabilization effect," *IEEE Access*, vol. 7, pp. pp81246–81256, 2019.

[8] K. Yi, L. Tang, H. Wei, Z. Zhang, R. Hu, and K. Luo, "A mixed equilibrium model and optimal path platooning method for CAV platoons in heterogeneous traffic flow," *Journal of Advanced Transportation*, vol. 2023, Article ID 9370609, 11 pages, 2023.

[9] X. He and X. Wu, "Eco-driving advisory strategies for a platoon of mixed gasoline and electric vehicles in a connected vehicle system," *Transportation Research Part D: Transport and Environment*, vol. 63, pp. 907–922, 2018.

[10] S. Gong and L. Du, "Cooperative platoon control for a mixed traffic flow including human drive vehicles and connected and autonomous vehicles," *Transportation Research Part B: Methodological*, vol. 116, pp. 25–61, 2018.

[11] K. Long, C. Ma, Z. Jiang, Y. Wang, and X. Yang, "Integrated optimization of traffic signals and vehicle trajectories at intersection with the consideration of safety during signal change," *IEEE Access*, vol. 8, pp. 170732–170741, 2020.

[12] Z. Wang, G. Wu, and M.-J. Barth, "Cooperative eco-driving at signalized intersections in a partially connected and automated vehicle environment," *IEEE Transactions on Intelligent Transportation Systems*, vol. 21, no. 5, pp. 2029–2038, 2020.

[13] M. Pourmehrab, P. Emami, M. Martin-Gasulla, J. Wilson, L. Elefteriadou, and S. Ranka, "Signalized intersection performance with automated and conventional vehicles: a comparative study," *Journal of Transportation Engineering, Part A: Systems*, vol. 146, no. 9, 2020.

[14] A. Berbar, A. Gastli, N. Meskin et al., "Reinforcement learning-based control of signalized intersections having platoons," *IEEE Access*, vol. 10, pp. 17683–17696, 2022.

[15] M. Zhou, Y. Yu, and X. Qu, "Development of an efficient driving strategy for connected and automated vehicles at signalized intersections: a reinforcement learning approach," *IEEE Transactions on Intelligent Transportation Systems*, vol. 21, no. 1, pp. 433–443, 2020.

[16] Z. Yao, Y. Wang, B. Liu, B. Zhao, and Y. Jiang, "Fuel consumption and transportation emissions evaluation of mixed traffic flow with connected automated vehicles and human-driven vehicles on expressway," *Energy*, vol. 230, Article ID 120766, 2021.

[17] Z. Nie and H. Farzaneh, "Real-time dynamic predictive cruise control for enhancing eco-driving of electric vehicles, considering traffic constraints and signal phase and timing (SPaT) information, using artificial-neural-network-based energy consumption model," *Energy*, vol. 241, Article ID 122888, 2022.

[18] J. Liu and X. Zuo, "Research on fuzzy control and optimization for traffic lights at single intersection," *Journal of System Simulation*, vol. 32, no. 12, pp. 2401–2408, 2020.

[19] B. K. Xiong, R. Jiang, and X. Li, "Managing merging from a CAV lane to a human-driven vehicle lane considering the uncertainty of human driving," *Transportation Research Part C: Emerging Technologies*, vol. 142, Article ID 103775, 2022.

[20] B. Xu, X. J. Ban, Y. Bian et al., "Cooperative method of traffic signal optimization and speed control of connected vehicles at isolated intersections," *IEEE Transactions on Intelligent Transportation Systems*, vol. 20, no. 4, pp. 1390–1403, 2019.